Journal of Manufacturing Processes 68 (2021) 1114–1122

Contents lists available at ScienceDirect

Journal of Manufacturing Processes

journal homepage: www.elsevier.com/locate/manpro

On the transformation between micro-concave and micro-convex in nanosecond laser ablation of a Zr-based metallic glass

Yongfeng Qian [a], Minqiang Jiang [b,c], Zhiyu Zhang [d], Hu Huang [a,*], Jiwang Yan [e]

[a] Key Laboratory of CNC Equipment Reliability, Ministry of Education, School of Mechanical and Aerospace Engineering, Jilin University, Changchun, Jilin 130022, China
[b] State Key Laboratory of Nonlinear Mechanics, Institute of Mechanics, Chinese Academy of Sciences, Beijing 100190, China
[c] School of Engineering Science, University of Chinese Academy of Sciences, Beijing 100049, China
[d] Key Laboratory of Optical System Advanced Manufacturing Technology, Changchun Institute of Optics, Fine Mechanics and Physics, Chinese Academy of Sciences, Changchun, China
[e] Department of Mechanical Engineering, Faculty of Science and Technology, Keio University, Yokohama 223-8522, Japan

ARTICLE INFO

Keywords:
Laser ablation
Metallic glass
Microstructure formation
Transformation
Surface patterning

ABSTRACT

Understanding the physical mechanism of laser-material interaction is significant and meaningful in both pure science and engineering applications. Laser ablation induced micro-concave is a commonly-observed phenomenon, but the formation of micro-convex by laser ablation is rarely reported. In this study, the transformation in surface microstructure from micro-concave to micro-convex, then to micro-concave again was reported for the first time in laser ablation of a typical Zr-based metallic glass (MG). The experimental results indicated that such transformations strongly depended on the peak laser power intensity and number of laser pulses. The coupling effects of the recoil pressure and Marangoni flow were proposed to explain the observed transformation. By locally overlapping adjacent micro-convexes, various surface patterns could be fabricated on the MG surface, which could tune its surface wettability. This study would not only enhance the understanding of laser-MG interaction but also provide new methods for patterning MG surface.

1. Introduction

Laser ablation of materials has many potential applications, such as laser additive manufacturing [1–5], laser shock peening [6–8], and laser surface patterning [9–13]. Apart from these practical engineering applications, the scientific community is also fascinated by laser-material interaction as well as the underlying physics and thermodynamics [14,15]. In laser ablation process, the laser beam will create a local molten pool on the material surface. This molten pool will deform with the role of recoil pressure and surface tension during the subsequent solidification process, resulting in various micro/nano-scale surface structures [16,17]. Generally, after ablation by single/multi-pulse laser with Gaussian energy distribution, a typical micro-concave would be formed on the material surface due to the recoil pressure caused by rapid vaporization [18,19]. In contrast, only very few studies [20,21] have reported the formation of micro-convex on some specific materials due to the effect of surface tension. Actually, as the two most dominant driving forces, recoil pressure and surface tension generally coexist during laser ablation process, in a competitive or cooperative way determined by applied laser ablation parameters and the properties of materials. However, most of the current studies generally only study the individual role of these two driving forces, and their coupling effects are ignored.

One of the key issues in understanding the complex laser-material interaction is to properly select the target materials. Taking features of metastability [22,23], thermal sensitivity [22,24], isotropy [25], and being free of defects and grain boundary [26–29], metallic glasses (MGs) provide a promising choice for further exploring the interaction between the laser beam and material. It has been found that micro-concave could be generated on the MG surface after single/multi pulse laser ablation [30,31]. However, to our knowledge, the detailed topographical transformation in nanosecond pulsed laser ablation of MGs has not been studied. Moreover, for MGs, it is still not clear whether micro-convex can be formed by direct laser ablation. Therefore, further exploration on laser ablation of MGs is required.

In this study, by multi-pulse nanosecond laser ablation of Zr-based

* Corresponding author.
E-mail address: huanghu@jlu.edu.cn (H. Huang).

https://doi.org/10.1016/j.jmapro.2021.06.034
Received 25 May 2021; Received in revised form 14 June 2021; Accepted 17 June 2021
Available online 29 June 2021

MG surface, the transformation from micro-concave to micro-convex, then to micro-concave again was achieved for the first time in the field of MGs. It was found that the formation of surface microstructure significantly depended on the applied peak laser power intensity (I) and the number of laser pulses (N). The coupling effects of the recoil pressure and Marangoni flow were proposed to explain the observed transformation.

2. Materials and experiments

The raw material used in experiments is a representative MG, $Zr_{41.2}Ti_{13.8}Cu_{12.5}Ni_{10}Be_{22.5}$ (at.%, Vit 1) with a dimension of 20 mm × 20 mm × 2 mm. To obtain a mirror-like surface, the sample was ground and polished in sequence. The amorphous characteristic of the sample was verified by X-ray diffraction (XRD) before laser ablation. A fiber nanosecond pulsed laser (SP-050P-A-EP-Z-F-Y, SPI Lasers, UK) with wavelength of 1064 nm, pulse duration of 7 ns, and repetition frequency of 800 kHz was utilized for multi-pulse laser ablation of MG sample. The laser beam has a Gaussian energy distribution ($M^2 < 2$) and it is focused to be a spot with diameter of about 43 μm. To investigate the evolution of laser-induced surface microstructure, two groups of comparative experiments were performed, one keeping the number of laser pulses constant and changing the peak laser power intensity, and the other keeping the peak laser power intensity constant and changing the number of laser pulses. To avoid crystallization and oxidation, all the experiments were conducted in high purity argon gas with a pressure of 0.01 MPa. After laser ablation, the surface characteristics of the ablated regions were measured by a laser scanning confocal microscope (LSCM, OLS4100, Olympus, Japan) and an optical microscope (OM, DSX500, Olympus, Japan). The surface wettability was characterized by an optical surface analyser (OSA60, LAUDA Scientific, Germany).

3. Results

Figs. 1(a)–(d) present the 3D topographies of the ablated regions obtained at the same number of laser pulses (N = 1000) but under various peak laser power intensities, $I = 2.4 \times 10^{11}$ W/m^2 (Fig. 1(a)), $I = 3.6 \times 10^{11}$ W/m^2 (Fig. 1(b)), $I = 2 \times 10^{12}$ W/m^2 (Fig. 1(c)), and $I = 3.6 \times 10^{12}$ W/m^2 (Fig. 1(d)). The corresponding cross-sectional profiles marked in Figs. 1(a)–(d) are illustrated in Figs. 1(e)–(h), respectively. The topographical evolution in Figs. 1(a)–(h) directly indicates that the laser-induced surface microstructure greatly depends on the applied peak laser power intensity. At a relatively low peak laser power intensity of 2.4×10^{11} W/m^2, a typical micro-concave with depth of about 640 nm is generated. When increasing the peak power intensity to 3.6×10^{11} W/m^2, the resultant surface microstructure is still a micro-concave on the whole, but surprisingly, the depth of the concave does not increase and its bottom is almost on the same height with the original polished surface as shown in Fig. 1(f). Further increasing the peak laser power intensity to 2×10^{12} W/m^2, a micro-convex with diameter of about 165 μm is formed on the MG surface, rather than the previously observed micro-concave. On the top of the micro-convex, there is a micro-concave and the height from its bottom to the original polished surface is about 400 nm. When further increasing the peak laser power intensity for example to 3.6×10^{12} W/m^2, the surface microstructure is transformed into micro-concave again as shown in Fig. 1(d). Since the relative position of the bottom of the micro-concave and the original polished surface determines whether the surface microstructure is concave or convex, their height difference is used to quantitatively study the correlation between the surface microstructure and the peak laser power intensity. The height differences are averaged after five experiments, and the corresponding results are depicted in Fig. 1(i). It is clear that as the peak laser power intensity increases, the height difference gradually changes from negative to positive, reaches the maximum value of about 400 nm, and then gradually becomes negative again after keeping the height nearly constant in the range of 1×10^{12} to 1.8×10^{12} W/m^2. This demonstrates that the surface microstructure changes from micro-concave to micro-convex, and then to micro-concave again. In addition, it is noted that with increase in peak laser power intensity, the diameter of the laser-induced surface microstructure gradually increases as shown in Fig. 1(j). This is due to that increasing the peak laser power intensity, more heat diffuses to the surface and inside of the MG, resulting in a larger ablated region. The results in Fig. 1 confirm the fact that changing the peak laser power intensity, the laser-induced surface microstructure will transform from micro-concave to micro-convex, then to micro-concave again.

Next, the effects of the number of laser pulses on the evolution of surface microstructure are investigated at a constant peak laser power intensity of 1×10^{12} W/m^2, but under various numbers of laser pulses. Fig. 2 presents the results. In Figs. 2(a) and (e), where the number of laser pulses is relatively small (N = 50), a relatively shallow micro-concave with pileup around is formed in the ablated region. When the number of laser pulses increases to 200, a micro-convex with a very low height (about 20 nm) is formed, as shown in Figs. 2(b) and (f). When the number of laser pulses further increases to 100,000, the height value increases to 1250 nm, which is almost three times of the maximum height obtained when changing the peak laser power intensity. When the number of laser pulses reaches 5,000,000, the micro-concave appears again. As shown in Figs. 2(i) and (j), the statistical results of the height difference and diameter obtained when increasing the number of laser pulses are quite similar to those obtained when increasing the peak laser power intensity as shown in Figs. 1(i) and (j). That is, the height difference changes from negative to positive, and then to negative again, but the diameter gradually increases. In addition, when increasing the number of laser pulses from 50,000 to 100,000, there is also a holding stage that the height value basically keeps constant. The results in Figs. 1 and 2 indicate that increasing either the peak laser power intensity or the number of laser pulses has almost the similar influence on the evolution of the surface microstructure, and both of them could induce the transformation in surface microstructure between the micro-concave and micro-convex.

4. Discussion

4.1. Microstructure transformation mechanism

According to the above results, laser ablation of Zr-based MG in argon gas could result in the transformation in surface microstructure between the micro-concave and micro-convex when increasing the peak laser power intensity and number of laser pulses. Previous study [32] indicated that surface characteristics of MG after laser ablation may vary when changing the gas atmosphere. Therefore, to exclude the influence of gas atmosphere, similar experiments were also conducted in nitrogen gas and air, and the same microstructure transformation was also observed (not shown here). This confirms that laser-induced transformation in surface microstructure of MG is a universal phenomenon, independent of the ablation atmosphere. To explain this transformation, Fig. 3 illustrates the possible mechanism. During laser ablation, a local molten pool would be formed on the MG surface. At a relatively low peak laser power intensity and number of laser pulses, the alloy melt in the center of the molten pool would flow outside with the role of recoil pressure generated due to rapid vaporization, leading to the formation of typical micro-concave. When gradually increasing the peak laser power intensity and number of laser pulses, the dominant driving force of the alloy melt may change to the surface tension [21]. For alloys with a fixed element composition, surface tension is directly related to the temperature [17,33]. However, the surface tension of Vit 1 at high temperature is quite difficult to measure due to the high viscosity of its melt [34] and the highly active elements it contains (Zr, Ti and Ni) [35]. Generally, the bond between two atoms decreases when increasing the temperature, resulting in a negative surface tension coefficient [36,37]. However, it has been proved that [38] for some multi-element alloy

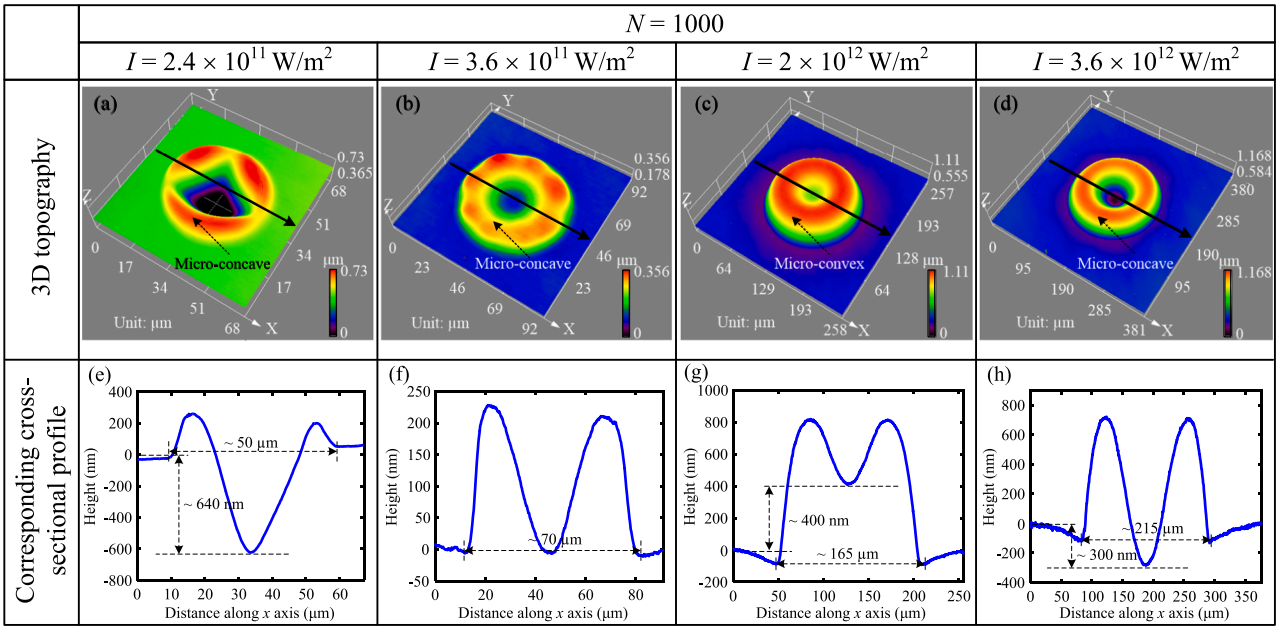

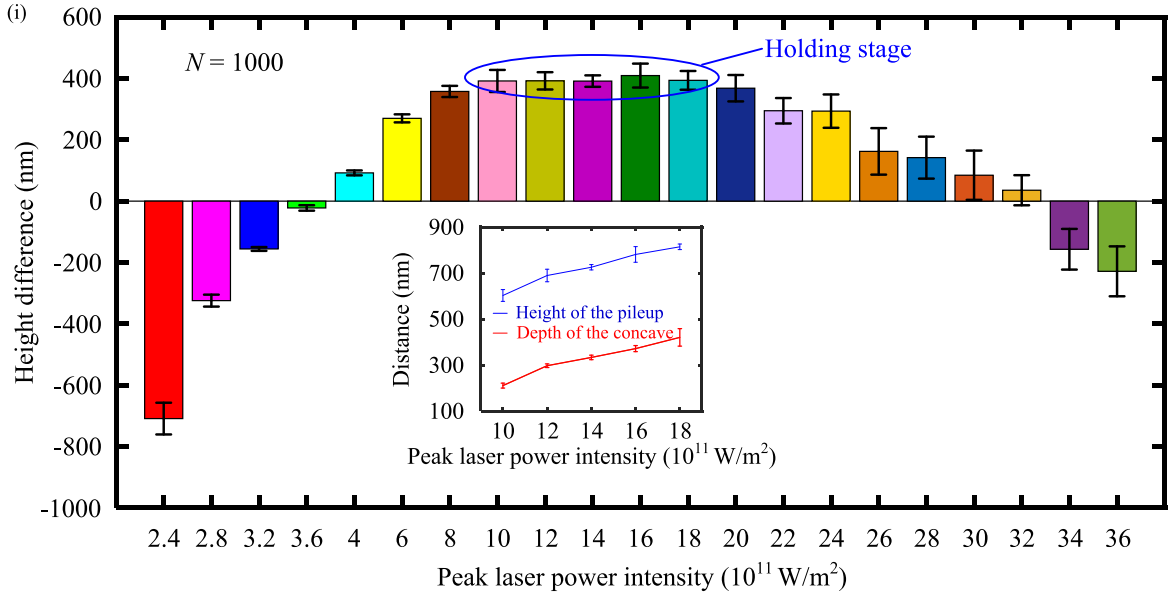

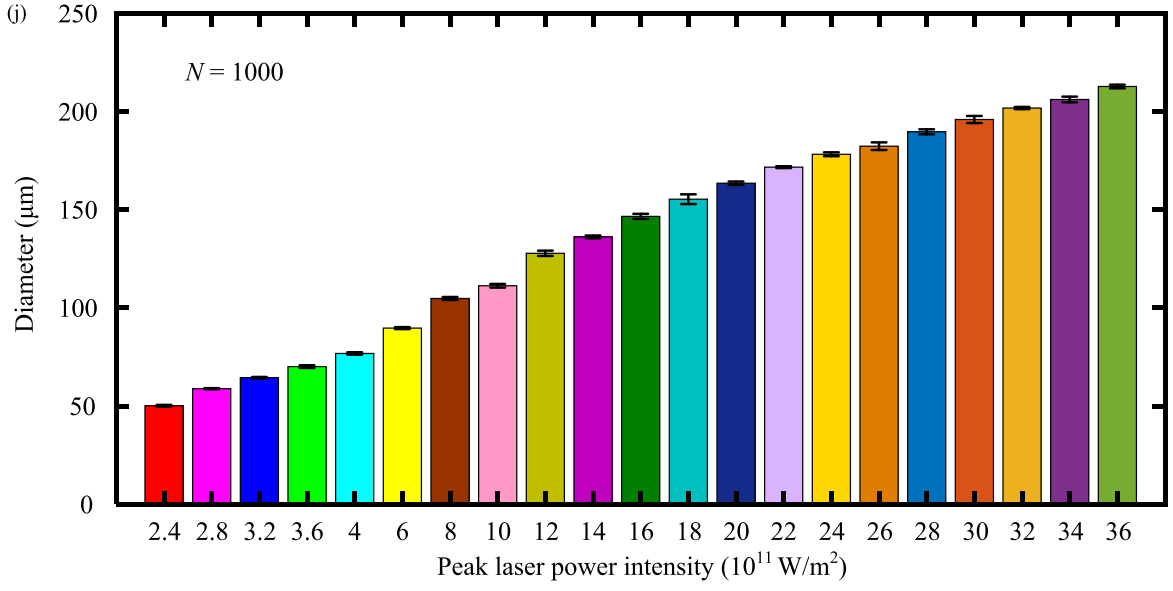

(caption on next page)

Fig. 1. 3D topographies of the laser ablated regions obtained at various peak laser power intensities: (a) $I = 2.4 \times 10^{11}$ W/m^2, (b) $I = 3.6 \times 10^{11}$ W/m^2, (c) $I = 2 \times 10^{12}$ W/m^2, and (d) $I = 3.6 \times 10^{12}$ W/m^2. (e)–(h) Cross-sectional profiles of the marked lines in Figs. 1(a)–(d). (i) Effect of the peak laser power intensity on the height difference between the bottom of the micro-concave and the original polished surface. (j) Effect of the peak laser power intensity on the diameter of laser-induced microstructure. For all these experiments, the number of laser pulses is kept to be 1000.

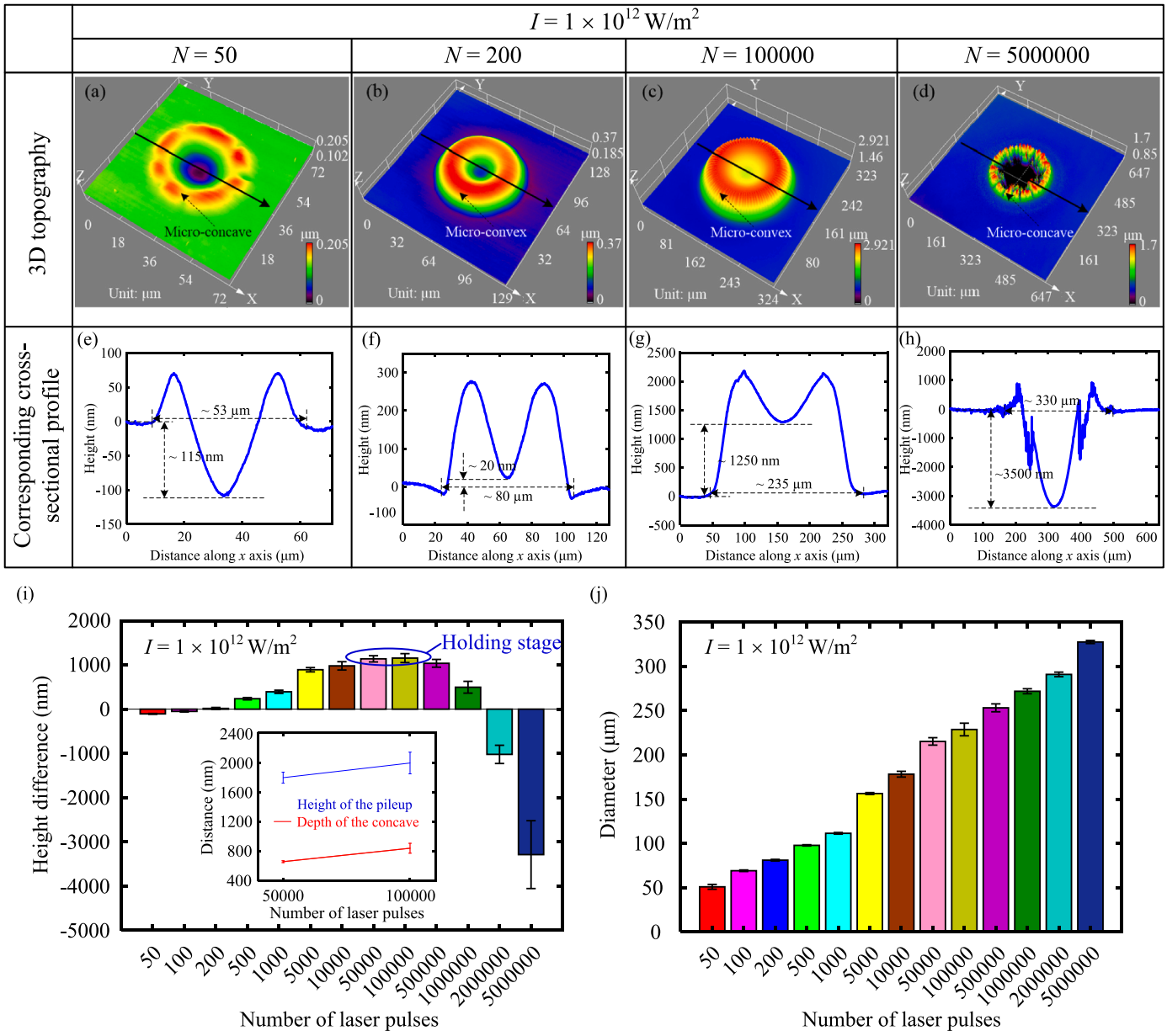

Fig. 2. 3D topographies of the laser ablated regions at various numbers of laser pulses: (a) $N = 50$, (b) $N = 200$, (c) $N = 100{,}000$, and (d) $N = 5{,}000{,}000$. (e)–(h) Cross-sectional profiles of the marked lines in Figs. 2(a)–(d). (i) Effect of number of laser pulses on the height difference between the bottom of the micro-concave and the original polished surface. (j) Effect of number of laser pulses on the diameter of laser-induced microstructure. For all these experiments, the peak laser power intensity is kept to be 1×10^{12} W/m^2.

systems, when they are heated to a critical temperature, the surface tension coefficient might change from the negative to the positive owing to dissolution and re-distribution of clusters. In addition, it was also reported that surface vaporization had a great influence on the surface tension and would further promote this change [39]. Accordingly, when the applied peak laser power intensity and number of laser pulses are high enough to cause the temperature of almost the entire molten pool to exceed the critical temperature, the flow behavior of alloy melt would change significantly with the role of positive surface tension coefficient. As the laser beam has a Gaussian energy distribution, the center of the molten pool has the highest temperature and therefore the maximum surface tension, which results in radially inward flow (i.e. Marangoni flow) of alloy melt [17,36,40], forming the micro-convex as shown in Figs. 1(c) and 2(c). At the same time, the recoil pressure caused by rapid vaporization would still create a small micro-concave on the top of the micro-convex. Specially, within a range of ablated parameters as illustrated in the insets of Figs. 1(i) and 2(i), the increase in the height of the pileup caused by Marangoni flow is almost in step with the increase in the depth of the small micro-concave caused by the recoil pressure, which leads to the appearance of the holding stage. In the above cases,

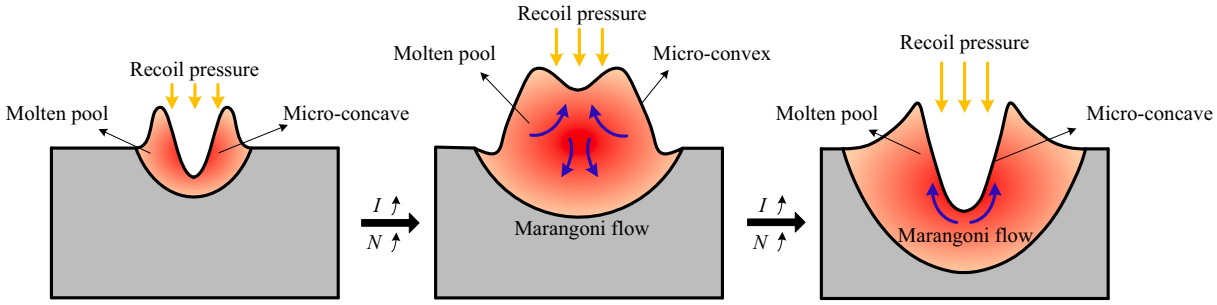

Fig. 3. The schematic diagram illustrating the transformation from micro-concave to micro-convex, then to micro-concave again when increasing the peak laser power intensity and the number of laser pulses.

the recoil pressure and Marangoni flow are in competition with each other. However, at a relatively high peak laser power intensity and number of pulses, their correlation may be changed to cooperation. As reported in many studies [20,36,41], the temperature-dependent surface tension coefficient is not always positive after exceeding the critical temperature, and it changes from positive to negative when another critical temperature is reached. At a relatively high peak laser power intensity and number of pulses, the temperature of the molten pool may exceed this critical temperature. In this case, the alloy melt will flow radially outward due to the negative surface tension coefficient, which could cause the Marangoni flow to cooperate with recoil pressure and thus promote the formation of micro-concave. From above analysis, the coupling effects of recoil pressure and Marangoni flow are the key to determine the final surface microstructure, concave or convex. At a relatively low peak laser power intensity and number of laser pulses, the dominant driving force is the recoil pressure, resulting in the formation of micro-concave; when gradually increasing the peak laser power intensity and number of laser pulses, the Marangoni flow is dominant, leading to the formation of micro-convex; while at a relatively high peak laser power intensity and number of laser pulses, the recoil pressure and Marangoni flow cooperate with each other, and the micro-concave is formed again.

Laser induced formation of the micro-concave is a commonly-observed phenomenon, and compared to the micro-concave, the observed micro-convex in this study is more interesting and attractive. For practical applications, the height of the micro-convex is an important parameter. From above results and analysis, it is noted that although the transformation process of the surface microstructure is the same when increasing the peak laser power intensity and number of laser pulses, the resultant maximum height of the micro-convex is relatively small by means of increasing the peak laser power intensity. This could be due to that the higher peak laser power intensity would induce a strong recoil pressure during the laser-MG interaction, which impedes the growth of the micro-convex to a certain extent. Corresponding to two different peak laser power intensities, Figs. 4(a) and (b) show the height of the pileup and the depth of the micro-concave on the top of the micro-convex changing with the number of laser pulses. It is found that for these two peak laser power intensities, both the height of the pileup and the depth of the micro-concave increase when increasing the number of laser pulses, which indicates that the Marangoni flow and the recoil pressure are continuously strengthened. Furthermore, for a fixed number of laser pulses, the height of the pileup and the depth of the micro-concave will increase when increasing the peak laser power intensity from 7.5×10^{11} to 1×10^{12} W/m^2. In fact, as illustrated in Fig. 4 (c), when increasing the peak laser power intensity, the size relationship between the height difference of the pileup (H_d) and the depth difference of the micro-concave on the top of the micro-convex ($D_2 - D_1$) determines the increase or decrease of the height of the micro-convex: if $H_d > D_2 - D_1$, the height of the micro-convex increases, and vice versa. Fig. 4(d) presents the distance difference including the height difference (H_d) and the depth difference ($D_2 - D_1$), changing with the number of laser pulses. At a relatively small number of laser pulses ($N = 2000$ and 5000), when increasing the peak laser power intensity from 7.5×10^{11} to 1×10^{12} W/m^2, the height difference of the pileup (H_d) is almost equal to the depth difference of the micro-concave on the top of the micro-convex ($D_2 - D_1$), so the height of the micro-convex is basically the same under these two peak laser power intensities, as shown in Fig. 4 (e). However, when the number of laser pulses reaches 10,000 or more, the height difference (H_d) is less than the depth difference ($D_2 - D_1$), and correspondingly, the height of the micro-convex is greater at a relatively low peak laser power intensity. In particular, when laser ablation is performed under the peak laser power intensity of 7.5×10^{11} W/m^2 and number of laser pulses of 10,000, the micro-convex shows an almost flat top, as shown in Figs. 4(f) and (g). The above results indicate that increasing the peak laser power intensity within a certain range will promote the Marangoni flow, but at the same time, a significant increase in recoil pressure will lead to the decrease in the height of the micro-convex.

4.2. Surface patterning

The above results indicate that within a wide range of ablated parameters, individual micro-convex with quite regular shape could be generated on the MG surface. However, for practical engineering applications, the line-shaped micro-convex structure is undoubtedly of great significance. Therefore, by locally overlapping adjacent micro-convexes, the possibility for fabricating the line-shaped micro-convex structure was verified. In order to avoid excessive local heat accumulation during the overlapping process, the employed peak laser power intensity and number of laser pulses were relatively low ($I = 7.5 \times 10^{11}$ W/m^2 and $N = 800$). Figs. 5(b)–(d) present the 3D topographies of the laser ablated regions under the overlap rates of 0%, 50% and 75%, respectively. From Figs. 5(c) and (d), it is seen that at a relatively high overlap rate, adjacent micro-convexes could be combined to form the line-shaped micro-convex structure. In addition, as shown in Figs. 5(h) and (j), when increasing the overlap rate from 50% to 75%, the height fluctuation of the line-shaped micro-convex structure along the overlapping direction is greatly reduced from about 250 nm to 75 nm. The above results demonstrate that our results can provide a new method for patterning MG surface. To further verify the flexibility of this method, the same ablated parameters were used to produce some special patterns, and Fig. 6 presents two typical surface patterns, the round and square micro-convex structures.

4.3. Surface wettability

Some previous studies [42,43] have demonstrated that surface microstructures would significantly affect the wettability of materials. To check the effect of the formed micro-convex structure on the surface wettability, a patterned MG surface with a regular array of micro-convexes was prepared (see Fig.7 (a)) using the same ablated parameters in Fig. 5, and its surface wettability was characterized by measuring

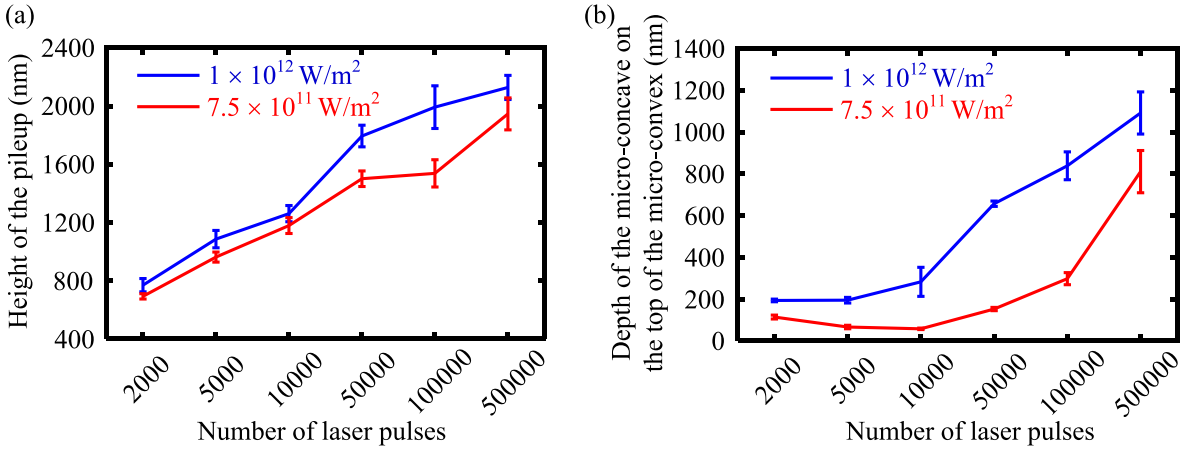

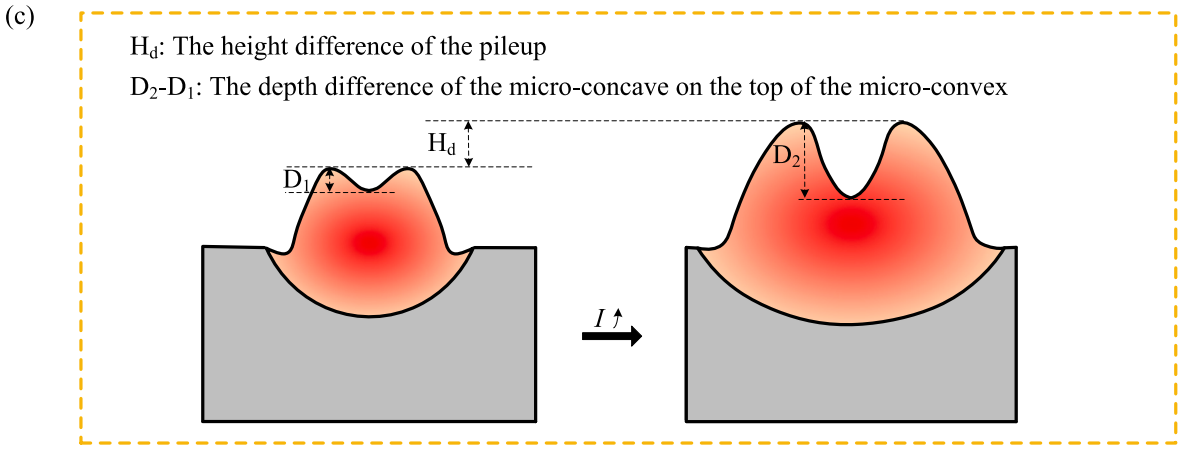

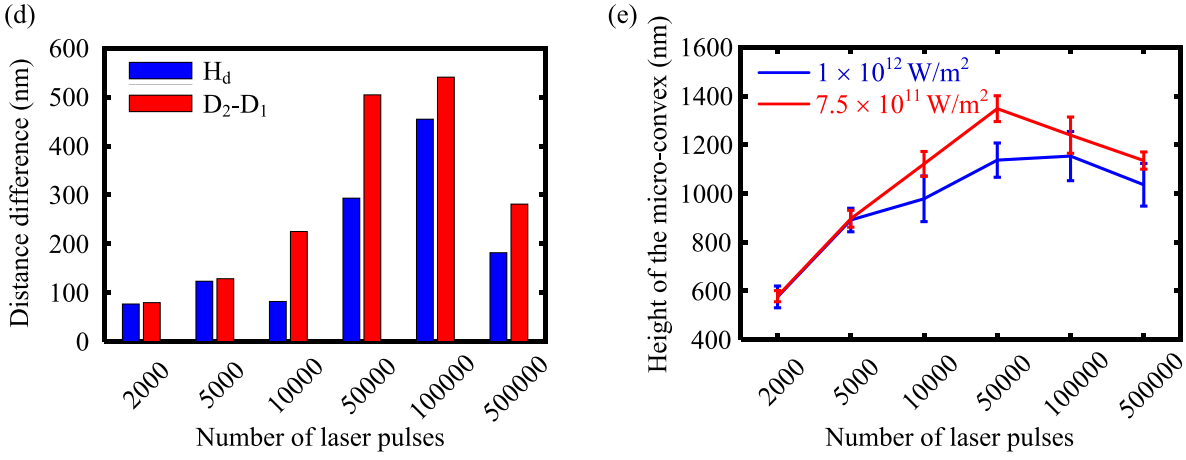

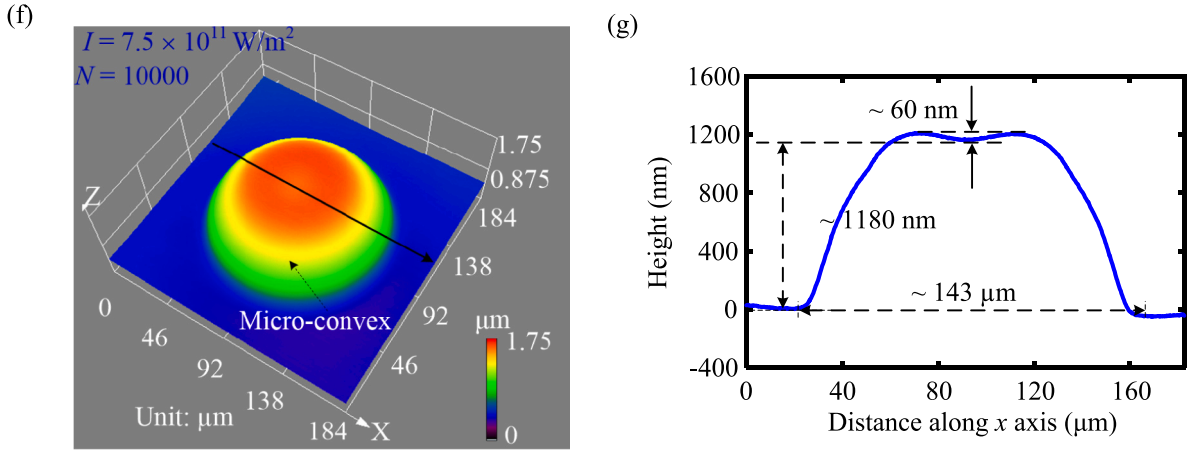

(caption on next page)

Fig. 4. (a) and (b) Effects of the peak laser power intensity and number of laser pulses on the height of the pileup and the depth of the micro-concave on the top of the micro-convex, respectively. (c) The schematic diagram illustrating how the size relationship between the height difference of the pileup (H_d) and the depth difference of the micro-concave on the top of the micro-convex ($D_2 - D_1$) determines the increase or decrease of the height of the micro-convex when increasing the peak laser power intensity. (d) The comparison in the height difference (H_d) and the depth difference ($D_2 - D_1$) between the micro-convexes obtained under two different peak laser power intensities and various numbers of laser pulses. (e) Effects of the peak laser power intensity and number of laser pulses on the height of the micro-convex. (f) 3D topography of the laser ablated region obtained under the peak laser power intensity of 7.5×10^{11} W/m^2 and number of laser pulses of 10,000. (g) Cross-sectional profile of the marked line in Fig. 4(f).

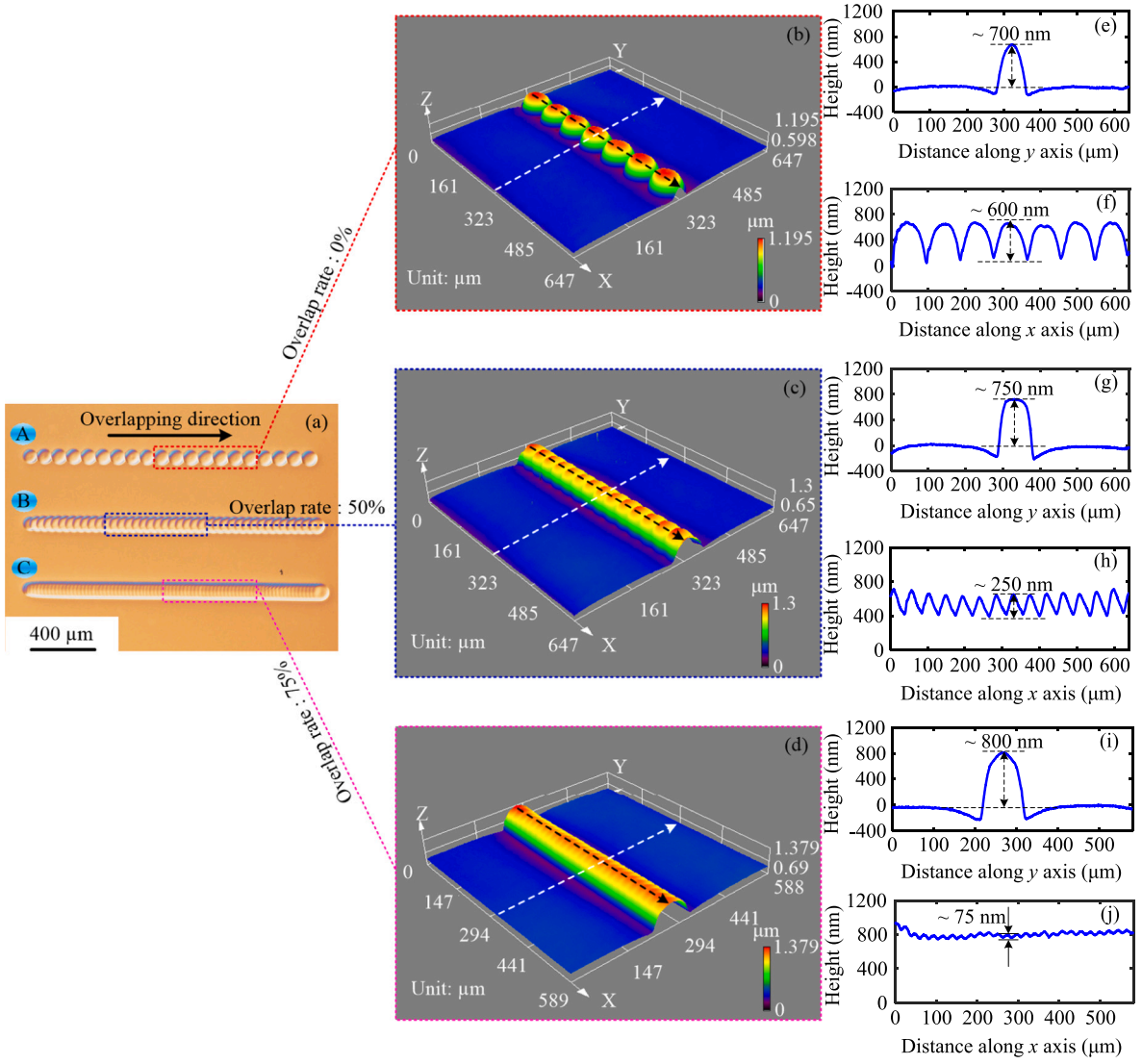

Fig. 5. (a) Optical image of the laser ablated regions obtained under different overlap rates (A: 0%, B: 50% and C: 75%). 3D topographies of the laser ablated regions obtained under different overlap rates: (b) 0%, (c) 50% and (d) 75%. (e) and (f) Cross-sectional profiles of the white dotted line and black dotted line in Fig. 5(b), respectively. (g) and (h) Cross-sectional profiles of the white dotted line and black dotted line in Fig. 5(c), respectively. (i) and (j) Cross-sectional profiles of the white dotted line and black dotted line in Fig. 5(d), respectively.

the contact angle (CA). The used liquid during testing was deionized water (5 μl in volume). For comparison, the CA of the polished surface was also tested and it is about 89.2° (see Fig. 7(c)). While, for the patterned MG surface with micro-convex array, the CA is reduced to 72.4° as shown in Fig. 7(d). In order to construct a superhydrophobic surface, the polished surface and the patterned surface were soaked in a 1.0 vol% fluoroalkylsilane solution for 2 h, and Figs. 7(e) and (f) show their CAs, respectively. After chemical modification, the CA of the polished surface is increased to 132.8°, exhibiting hydrophobicity. In Fig. 7 (f), the CA of the patterned surface is significantly increased to 158.7° after chemical modification, demonstrating superhydrophobicity. These results indicate that the introduction of micro-convex array would tune the surface wettability of MG, which provides potential interest for practical engineering applications of MGs, such as self-cleaning and directional droplet transport. In addition, it should be pointed out that the ablation parameters used here are not optimized, and further optimization will be performed in the future to study the effects of the generated microstructure on the optical and tribological properties of MGs.

5. Conclusions

In summary, nanosecond pulsed laser ablation induced surface microstructural evolution of Zr-based MG was investigated. The

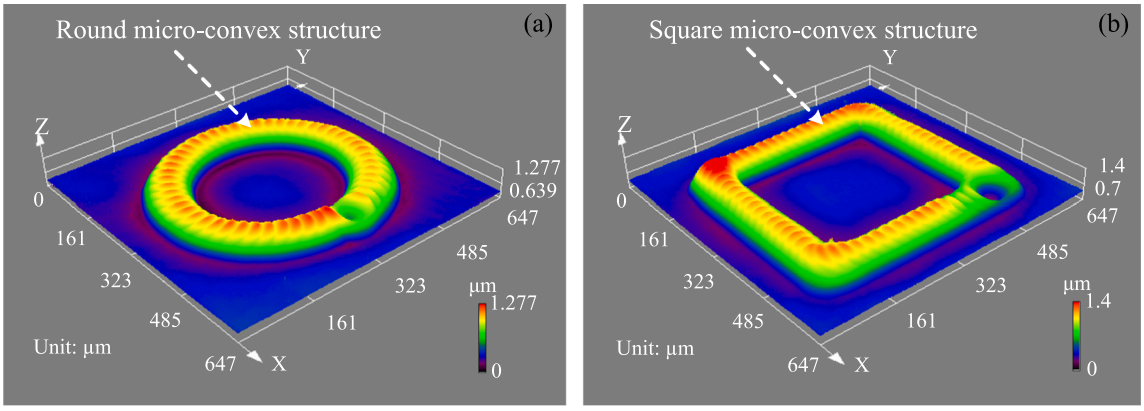

Fig. 6. 3D topographies of (a) round and (b) square micro-convex structures fabricated by laser ablation.

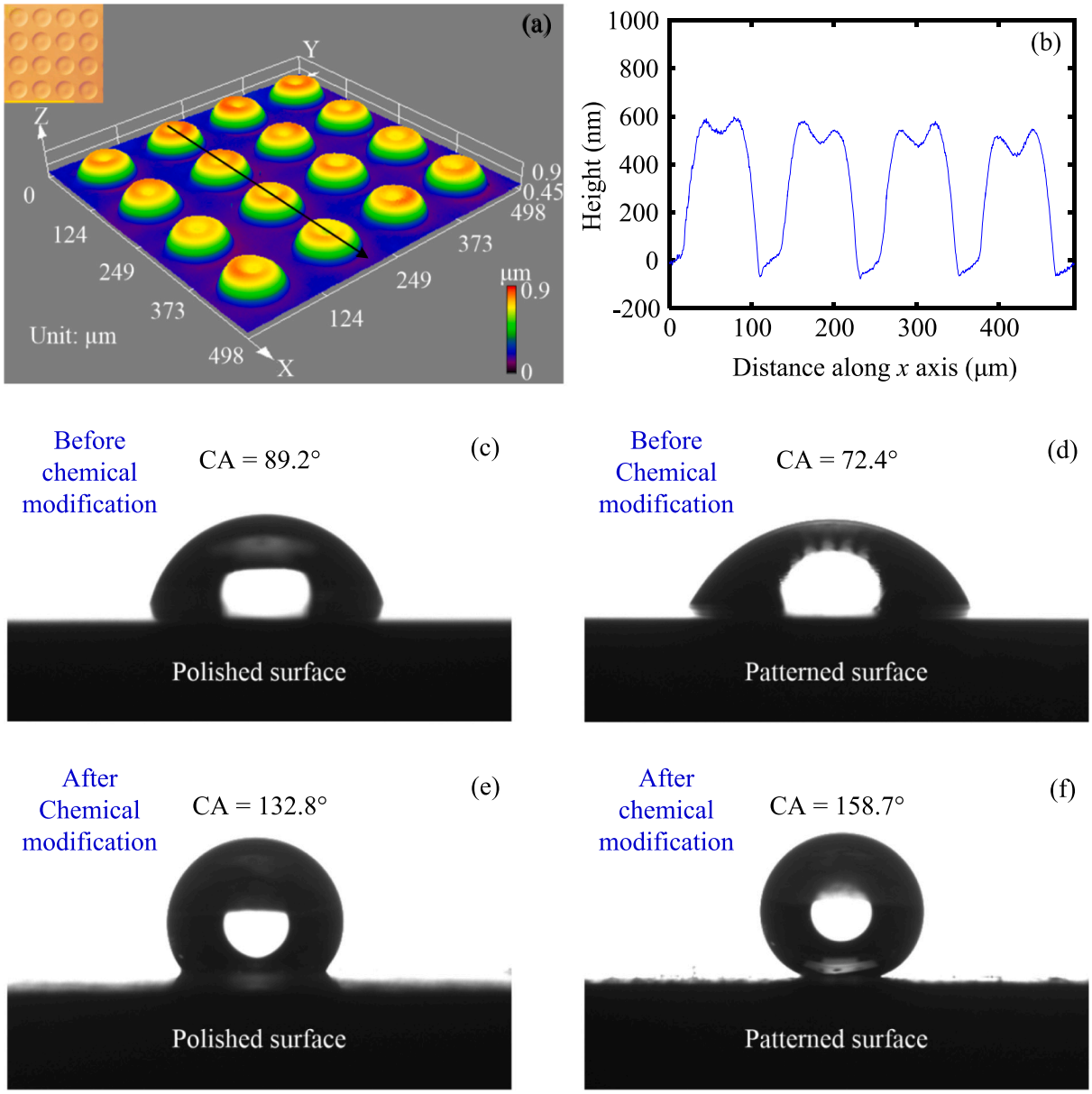

Fig. 7. (a) 3D topography of the laser ablated regions with a regular array of micro-convexes. The inset shows the corresponding optical morphology. (b) Cross-sectional profile of the marked line in Fig. 7(a). (c) and (e) show the water droplets on the polished surface before and after chemical modification. (d) and (f) show the water droplets on the patterned surface before and after chemical modification.

transformation in surface microstructure between the micro-concave and micro-convex was observed, which strongly depended on the peak laser power intensity and number of laser pulses. For a given number of laser pulses (or peak laser power intensity), when gradually increasing the peak laser power intensity (or number of laser pulses), the surface microstructure would transform from micro-concave to micro-convex, then to micro-concave again. The coupling effects of the recoil pressure and Marangoni flow were proposed to explain the observed transformation. By locally overlapping adjacent micro-convexes, several patterned surfaces with micro-convex structure were successfully fabricated. The patterned MG surface with a regular array of micro-convexes showed superhydrophobicity after chemical modification. These results are expected to enhance the understanding of complex laser-material interaction and as well provide a new method to pattern MGs for improving their functional applications.

Data availability

The raw/processed data required to reproduce these findings cannot be shared at the time of submission due to technical or time limitations.

Declaration of competing interest

The authors declare that they have no known competing financial interests or personal relationships that could have appeared to influence the work reported in this paper.

Acknowledgements

This work was supported by the National Natural Science Foundation of China (Grant Nos. 51705197 and 11972315), the Young Elite Scientists Sponsorship Program by CAST(YESS) (Grant No. 2017QNRC001), the Graduate Innovation Fund of Jilin University (Grant No. 101832020CX106), and the Fundamental Research Funds for the Central Universities (2019-2021).

References

[1] Liu SY, Shin YC. Additive manufacturing of Ti6Al4V alloy: a review. Mater Des 2019;164:107552.
[2] Mahbooba Z, Thorsson L, Unosson M, Skoglund P, West H, Horn T, et al. Additive manufacturing of an iron-based bulk metallic glass larger than the critical casting thickness. Appl Mater Today 2018;11:264–9.
[3] Li YQ, Shen YY, Leu MC, Tsai HL. Building Zr-based metallic glass part on Ti-6Al-4V substrate by laser-foil-printing additive manufacturing. Acta Mater 2018;144:810–21.
[4] Lamichhane TN, Sethuraman L, Dalagan A, Wang H, Keller J, Paranthaman MP. Additive manufacturing of soft magnets for electrical machines—a review. Mater Today Phys 2020;15:100255.
[5] Lough CS, Escano LI, Qu ML, Smith CC, Landers RG, Bristow DA, et al. In-situ optical emission spectroscopy of selective laser melting. J Manuf Process 2020;53:336–41.
[6] Zhu YH, Fu J, Zheng C, Ji Z. Effect of laser shock peening without absorbent coating on the mechanical properties of Zr-based bulk metallic glass. Opt Laser Technol 2015;75:157–63.
[7] Maawad E, Sano Y, Wagner L, Brokmeier HG, Genzel CH. Investigation of laser shock peening effects on residual stress state and fatigue performance of titanium alloys. Mater Sci Eng A 2012;536:82–91.
[8] Dhakal B, Swaroop S. Review: laser shock peening as post welding treatment technique. J Manuf Process 2018;32:721–33.
[9] Huang H, Yan JW. Surface patterning of Zr-based metallic glass by laser irradiation induced selective thermoplastic extrusion in nitrogen gas. J Micromech Microeng 2017;27:075007.
[10] Hwang YT, Guo CL. Femtosecond laser-induced asymmetric large scale waves on gold surfaces. Appl Phys Lett 2012;101:021901.
[11] Chen XZ, Li X, Zuo P, Liang MS, Li XJ, Xu CY, et al. Three-dimensional maskless fabrication of bionic unidirectional liquid spreading surfaces using a phase spatially shaped femtosecond laser. ACS Appl Mater Interfaces 2021;13:13781–91.
[12] Gries T, Catrin R, Migot S, Soldera F, Endrino JL, Landa-Canovas AR, et al. Local modification of the microstructure and electrical properties of multifunctional Au-YSZ nanocomposite thin films by laser interference patterning. ACS Appl Mater Interfaces 2014;6:13707–15.
[13] Long JY, Fan PX, Gong DW, Jiang DF, Zhang HJ, Li L, et al. Superhydrophobic surfaces fabricated by femtosecond laser with tunable water adhesion: from lotus leaf to rose petal. ACS Appl Mater Interfaces 2015;7:9858–65.
[14] Harzic RL, Dörr D, Sauer D, Stracke F, Zimmermann H. Generation of high spatial frequency ripples on silicon under ultrashort laser pulses irradiation. Appl Phys Lett 2011;98:211905.
[15] Liu Y, Jiang MQ, Yang GW, Guan YJ, Dai LH. Surface rippling on bulk metallic glass under nanosecond pulse laser ablation. Appl Phys Lett 2011;99:191902.
[16] Huang H, Jun N, Jiang MQ, Ryoko M, Yan JW. Nanosecond pulsed laser irradiation induced hierarchical micro/nanostructures on Zr-based metallic glass substrate. Mater Des 2016;109:153–61.
[17] Du D, He YF, Sui B, Xiong LJ, Zhang H. Laser texturing of rollers by pulsed Nd:YAG laser. J Mater Process Technol 2005;161:456–61.
[18] Li KM, Yao ZQ, Hu YX, Gu WB. Friction and wear performance of laser peen textured surface under starved lubrication. Tribol Int 2014;77:97–105.
[19] Dai FZ, Wen DP, Zhang YK, Lu JZ, Ren XD, Zhou JZ. Micro-dimple array fabricated on surface of Ti6Al4V with a masked laser ablation method in air and water. Mater Des 2015;84:178–84.
[20] Wang XS, Zhang YN, Wang L, Xian JY, Jin MF, Kang M. Fabrication of micro-convex domes using long pulse laser. Appl Phys A 2016;123:51.
[21] Vilhena LM, Sedlaček M, Podgornik B, Vižintin J, Babnik A, Možina J. Surface texturing by pulsed Nd:YAG laser. Tribol Int 2009;42:1496–504.
[22] Jiang MQ, Wei YP, Wilde G, Dai LH. Explosive boiling of a metallic glass superheated by nanosecond pulse laser ablation. Appl Phys Lett 2015;106:021904.
[23] Kosiba K, Scudino S, Kobold R, Kühn U, Greer AL, Eckert J, et al. Transient nucleation and microstructural design in flash-annealed bulk metallic glasses. Acta Mater 2017;127:416–25.
[24] Huang H, Yan JW. Laser patterning of metallic glass. Micro/Nano Technol 2018;1:1–29.
[25] Kumar G, Tang HX, Schroers J. Nanomoulding with amorphous metals. Nature 2009;457:868–72.
[26] Yavari AR, Lewandowski JJ, Eckert J. Mechanical properties of bulk metallic glasses. MRS Bull 2007;32:635–8.
[27] Lu YZ, Su S, Zhang SB, Huang YJ, Qin ZX, Lu X, et al. Controllable additive manufacturing of gradient bulk metallic glass composite with high strength and tensile ductility. Acta Mater 2021;206:116632.
[28] Thurnheer P, Maaß R, Laws KJ, Pogatscher S, Löffler JF. Dynamic properties of major shear bands in Zr–Cu–Al bulk metallic glasses. Acta Mater 2015;96:428–36.
[29] Wang Q, Liu JJ, Ye YF, Liu TT, Wang S, Liu CT, et al. Universal secondary relaxation and unusual brittle-to-ductile transition in metallic glasses. Mater Today 2017;20:293–300.
[30] Jiao Y, Brousseau E, Shen XX, Wang XX, Han QQ, Zhu HX, et al. Investigations in the fabrication of surface patterns for wettability modification on a Zr-based bulk metallic glass by nanosecond laser surface texturing. J Mater Process Technol 2020;283:116714.
[31] Jiao Y, Brousseau E, Han QQ, Zhu HX, Bigot S. Investigations in nanosecond laser micromachining on the $Zr_{52.8}Cu_{17.6}Ni_{14.8}Al_{9.9}Ti_{4.9}$ bulk metallic glass: experimental and theoretical study. J Mater Process Technol 2019;273:116232.
[32] Huang H, Noguchi J, Yan JW. Shield gas induced cracks during nanosecond-pulsed laser irradiation of Zr-based metallic glass. Appl Phys A 2016;122:881.
[33] M'chaar R, Sabbar A, Moudane ME. Temperature dependences of surface tension, density and viscosity study of Sn-Ag-Cu with Bi additions using theoretical models. Sci Rep 2019;9:14177.
[34] Way C, Shaw T, Wadhwa P, Busch R. Shear rate dependence of viscosity and configurational entropy of the $Zr_{41.2}Ti_{13.8}Cu_{12}.5Ni_{10.0}Be_{22.5}$ metallic glass forming liquid. J Alloys Compd 2007;434-435:88–91.
[35] Mukherjee S, Johnson WL, Rhim WK. Noncontact measurement of high-temperature surface tension and viscosity of bulk metallic glass-forming alloys using the drop oscillation technique. Appl Phys Lett 2005;86:014104.
[36] Zhou J, Shen H, Pan YQ, Ding XH. Experimental study on laser microstructures using long pulse. Opt Lasers Eng 2016;78:113–20.
[37] Kou HB, Li WG, Zhang XY, Xu ND, Zhang XH, Shao JX, et al. Temperature-dependent coefficient of surface tension prediction model without arbitrary parameters. Fluid Phase Equilib 2019;484:53–9.
[38] Li Y, W-z Chen, B-s Dong, S-x Zhou. Effects of phosphorus and carbon content on the surface tension of FeSiBPC glass-forming alloy melts. J Non Cryst Solids 2018;496:13–7.
[39] Xue XM, Wang JT. The surface tension and composition of liquid FeP alloys. J Non Cryst Solids 1993;156-158:841–4.
[40] Le T-N, Lo Y-L. Effects of sulfur concentration and Marangoni convection on melt-pool formation in transition mode of selective laser melting process. Mater Des 2019;179:107866.
[41] Sharma S, Mandal V, Ramakrishna SA, Ramkumar J. Numerical simulation of melt pool oscillations and protuberance in pulsed laser micro melting of SS304 for surface texturing applications. J Manuf Process 2019;39:282–94.
[42] Xia T, Li N, Wu Y, Liu L. Patterned superhydrophobic surface based on Pd-based metallic glass. Appl Phys Lett 2012;101:081601.
[43] Wang C, Huang H, Qian YF, Zhang ZY, Yan JW. One-step fabrication of regular hierarchical micro/nano-structures on glassy carbon by nanosecond pulsed laser irradiation. J Manuf Process 2021;62:108–18.